Extinction dynamics of a discrete population in an oasis

Stefano Berti
Laboratoire de Mécanique de Lille, CNRS/UMR 8107, Université Lille 1, 59650 Villeneuve d'Ascq, France

Massimo Cencini
Istituto dei Sistemi Complessi, CNR, Via dei Taurini 19, 00185, Rome, Italy

Davide Vergni*
Istituto per le Applicazioni del Calcolo, CNR, Via dei Taurini 19, 00185, Rome, Italy

Angelo Vulpiani
Dipartimento di Fisica, Università "La Sapienza," Piazzale Aldo Moro 2, I-00185 Roma, Italy
and Istituto dei Sistemi Complessi, CNR, Via dei Taurini 19, 00185, Rome, Italy
(Received 12 March 2015; revised manuscript received 10 June 2015; published 29 July 2015)

Understanding the conditions ensuring the persistence of a population is an issue of primary importance in population biology. The first theoretical approach to the problem dates back to the 1950s with the Kierstead, Slobodkin, and Skellam (KiSS) model, namely a continuous reaction-diffusion equation for a population growing on a patch of finite size L surrounded by a deadly environment with infinite mortality, i.e., an oasis in a desert. The main outcome of the model is that only patches above a critical size allow for population persistence. Here we introduce an individual-based analog of the KiSS model to investigate the effects of discreteness and demographic stochasticity. In particular, we study the average time to extinction both above and below the critical patch size of the continuous model and investigate the quasistationary distribution of the number of individuals for patch sizes above the critical threshold.

DOI: 10.1103/PhysRevE.92.012722 PACS number(s): 87.10.Mn, 87.23.Cc

I. INTRODUCTION

Many biological or chemical processes involve the dynamics of discrete "particles" (e.g., molecules or organisms) that diffuse and interact with each other and/or with an external environment [1–7]. In population dynamics, for instance, individuals spread in space, interact, reproduce, and die.

If the number density of particles is very large, the macroscopic description in terms of continuous fields is typically appropriate. A well-established approach to model the spatiotemporal evolution of the population density field, $\mathcal{P}(x,t)$, is in terms of a reaction-diffusion equation that, in one spatial dimension, reads

$$\frac{\partial \mathcal{P}}{\partial t} = D\frac{\partial^2 \mathcal{P}}{\partial x^2} + f(\mathcal{P}). \tag{1}$$

In the above equation, D is the diffusion coefficient and $f(\mathcal{P})$ rules the chemical kinetics or, in the language of population biology, the local rate of population growth. A well-known growth term is the logistic model

$$f(\mathcal{P}) = r\mathcal{P}\left(1 - \frac{\mathcal{P}}{K}\right), \tag{2}$$

whose quadratic term models the competition for resources, K being the local carrying capacity (i.e., the maximal population density that can be sustained) while r denotes the intrinsic growth rate.

Conversely, if the density of particles is not very large the discrete nature of the population cannot be neglected [8], new effects arise, and the continuous description becomes inaccurate. In order to account for the new effects several approaches are possible. For instance, for a population of N individuals, a possibility is to introduce a cutoff at the value $1/N$ of the normalized density for the continuous field equations [9] (see Ref. [10] for a review). Another possibility is to supplement Eq. (1) with a noise term accounting for microscopic fluctuations originated by the finite number of individuals [11–13]. A further modeling step is to consider a lattice where each site is occupied by an integer number of individuals [14,15], or a contact process (see, e.g., Refs. [16,17] and references therein), where each site is occupied at most by an individual.

In the present work, we consider a system of particles diffusing in space and interacting when they get within a given interaction distance. In particular, revisiting the continuous Kierstead, Slobodkin, and Skellam (KiSS) model [18,19], we investigate the effects induced by discreteness on the dynamics of a population inhabiting a favorable region ("an oasis") surrounded by a deadly environment ("a desert"). Accounting for such effects is important to assess the role of demographic and environmental stochasticity on extinction dynamics [20].

Several efforts have already been undertaken along this direction within the framework of the KiSS model. Some model modifications that include effects of intrinsic variability on the critical habitat size ensuring population persistence have been studied in relation to environmental stochasticity [21]. As for demographic stochasticity due to population discreteness it has been investigated either using a cutoff on the continuous field equations [22], in the same spirit of Ref. [9], or within a stochastic framework using field-theory techniques [23]. In

*Corresponding author: davide.vergni@cnr.it

 ©2015 American Physical Society

our work, we adopt a discrete particle model [24] focusing on demographic stochasticity effects. Moreover, our study is not restricted to steady-state properties but also deals with dynamical features of extinction phenomena.

The article is organized as follows. In Sec. II we recall the continuous KiSS model [18,19] and introduce its discrete analog. In Sec. III we numerically study the long-time properties of the discrete model, characterizing the so-called quasistationary state [25,26], and compare it with the properties of the continuous model. Section IV is devoted to the problem of determining the critical habitat size for population persistence and to the estimation of extinction times in the discrete particle system. Discussions and conclusions are presented in Sec. V. As a side discussion, in the Appendix we briefly consider the effects of changes of the microscopic rules of the discrete model.

II. MODEL

A. Continuous KiSS model

Determining the conditions for persistence or, conversely, estimating the probability of the extinction of species and populations is a question of paramount importance in population biology. The theoretical treatment of the problem was initiated by Kierstead, Skellam, and Slobodkin [18,19], who considered a population that, ruled by Eqs. (1) and (2), grows with rate r and diffuses with diffusion coefficient D within a patch of size L surrounded by a deadly environment. For a given growth rate, higher diffusivities imply larger fluxes across the boundaries, so larger patches are necessary to compensate the population loss in order to allow stable persistence. It is then natural to determine the minimal (critical) patch size, L_c, ensuring population persistence. At least dimensionally, the critical patch size can be obtained by balancing the growth rate r with the exit rate from the patch due to diffusion D/L^2 [27]. This way one derives that $L_c \sim \sqrt{D/r}$ that is the correct result up to an order one constant (see below).

In one-dimensional space, for simplicity, it is enough to consider Eqs. (1) and (2) in the interval $0 \leqslant x \leqslant L$, representing the favorable patch, while the outside hostile environment results in the boundary conditions

$$\mathcal{P}(0) = \mathcal{P}(L) = 0. \tag{3}$$

Detailed analysis of the KiSS model can be found in Refs. [18,19,27–29]; for generalizations of the model including different kinds of population growth terms see Refs. [30,31]. Here we only recall the main results on the critical patch size. We notice that, close to extinction, the population density will be very small ($\mathcal{P} \ll K$) so we can linearize the growth term (2) by posing $f(\mathcal{P}) = r\mathcal{P}$. Starting from a generic initial condition, population density will thus grow (decay) depending on the positive (negative) sign of the largest eigenvalue λ_1 of the (linear) operator $\mathcal{L} = D\partial_x^2 + r$ with boundary conditions (3). Standard computation shows that the eigenvalues are

$$\lambda_n = r\left[1 - n^2\left(\frac{L_c}{L}\right)^2\right], \quad n = 1,2,\ldots, \tag{4}$$

with $L_c = \pi\sqrt{D/r}$. Consequently, the population can persist only if the favorable habitat is larger than the critical patch size L_c. However, while in the linear case also the eigenfunctions and thus the stationary population density can be easily derived, for the logistic case only approximate solutions are known (see, e.g., Ref. [18]).

It is worth noting that proper estimations of L_c, with suitable generalizations of the above model, are used in the design of protected areas for endangered species, in the context of conservation biology [32–34].

In the following we focus on the logistic growth case. For later convenience it is useful to formulate the continuous model [Eqs. (1) and (2)] in nondimensional variables. From the above analysis it is natural to measure time in units of the inverse growth rate $1/r$ and space in units of $\sqrt{D/r}$. Finally, normalizing the population density to the carrying capacity, which introduces $\theta = \mathcal{P}/K$, we can rewrite Eqs. (1) and (2) as

$$\frac{\partial\theta}{\partial t} = \frac{\partial^2\theta}{\partial x^2} + \theta(1-\theta), \tag{5}$$

with $\theta(0) = \theta(L) = 0$, where L now is the nondimensional domain size. With these units the critical patch size is $L_c = \pi$.

B. Discrete KiSS model

In recent years, much effort has been devoted to the extinction problem in populations with a finite number, N, of individuals, using nonspatial models [20,35–37]. The factors influencing extinction, through fluctuations and decline of a population, are in principle extremely varied and attributable to a wide class of biological and environmental causes, among which demographic stochasticity [37], associated to the unavoidable random occurrence of birth and death events, is one of the most important ones.

In the context of spatially extended systems, some effects of demographic stochasticity on steady patterns of populations have been analyzed using different models [22,23]. In particular, in Ref. [22] the discreteness was modeled using reaction-diffusion equations with a cutoff on the growth term, and it was found that the critical patch size for survival is larger than in the model without cutoff. A similar effect was found also in Ref. [23], using a stochastic discrete model, where it is shown that the population can go extinct above the critical patch size of the continuous model and an "effective" (finite) critical patch size can be introduced only when the competition term is weak enough. In our study, similarly to [22,23], the discrete population can go extinct for habitat sizes guaranteeing the persistence in the continuous case. However, we will always refer to the critical patch size of the continuous model L_c because, as we will see, this value still marks a transition in the system behavior.

We now introduce a discrete version of the KiSS model, generalizing the stochastic particle model of Ref. [24]. As an essential prerequisite, when the number of particles is large, the model must reproduce the Fisher-Kolmogorov-Petrovskii-Piskunov (FKPP) dynamics $\partial_t\theta = D\partial_x^2\theta + r\theta(1-\theta)$ [i.e., Eq. (5) in the dimensional version]. The FKPP equation can be derived from two coupled reaction-diffusion equations for the concentrations θ_A and θ_B of the species undergoing the

autocatalytic reaction

$$A + B \xrightarrow{r} 2B. \tag{6}$$

Summing the dynamical equation for θ_A ($\partial_t\theta_A = D_A\partial_x^2\theta_A - r\theta_A\theta_B$) with that for θ_B ($\partial_t\theta_B = D_B\partial_x^2\theta_B + r\theta_A\theta_B$) gives the FKPP equation, provided $D_A = D_B = D$ and $\theta_A + \theta_B = 1$ (i.e., local mass conservation). We discretize these reaction-diffusion equations passing from the concentrations $\theta_{A,B}$ to a particle description. Thus, we consider N_A particles of type A and N_B of type B, with $N = N_A + N_B$ fixed. All the particles undergo independent diffusive processes with the same diffusion coefficient, D, within the favorable patch $[0,L]$. Their positions x_α ($\alpha = 1,\ldots,N$) diffuse with diffusion coefficient D. As for the interaction between particles, a simple way to implement the interaction term $r\theta_A\theta_B$ is to impose that a particle of type A changes into B with a probability rate W_{AB} depending on the intrinsic rate, r, and on the number of B particles within an interaction distance R. This is mathematically formalized by the expression

$$W_{AB} = r\frac{n_B(x_\alpha;R)}{n_{\rm av}(R)} = r\frac{n_B(x_\alpha;R)}{2R\rho}, \tag{7}$$

where $n_B(x_\alpha;R)$ denotes the number of B particles within a distance R from the given A particle located at x_α and $n_{\rm av}(R) = 2R\rho$ the average number of particles (regardless of their type) within the interaction interval of length $2R$ ($\rho = N/L$ being the particle density). As discussed in Ref. [24], whenever the local particle density is large enough, the probabilistic rule above described converges to the FKPP equation. Finally, we have to fix the behavior of A and B particles at the boundaries. In order to reproduce the boundary conditions of the KiSS model and locally ensure mass conservation, we impose the following rules: A particles hitting the boundaries are reflected (nutrients are present only within the patch); if a B particle hits the boundary it is absorbed (as it cannot survive outside the favorable patch) and it is replaced in-place by an A particle.

The A particles are used as "auxiliary" ones in order to recover as a limit the continuous FKPP model. From an ecological perspective, considering A particles as nutrient, it would be interesting to study the case in which A and B particles diffuse with different diffusion coefficients. Clearly, in this case the FKPP equation cannot be the proper continuous description. Here we limit our discussion to the case of equal diffusion coefficients for the two species. In the Appendix, however, as an example we briefly consider the case of nondiffusing A particles (see also Fig. 1).

From the algorithmic point of view, the above model consists of two basic steps: the diffusive step, in which all particle positions x_α ($\alpha = 1,\ldots,N$) evolve according to the dynamics $dx_\alpha/dt = \sqrt{2D}\,\eta_\alpha$, with $\{\eta_\alpha\}$ independent normal random variables, and the reaction step, in which, for each A particle, one counts all the B particles within a distance R and changes A in B with probability $W_{AB}\Delta t$. Whenever the time step Δt is small enough the order in which the two steps are performed is irrelevant.

The main difference between the continuous model and the discrete one is that while the (continuous) stationary state $\theta = 0$ becomes unstable above the critical patch size, the (discrete) absorbing state $N_B = 0$ can always be reached due to demographic stochasticity. In the following sections we will investigate in depth this issue. Here we simply observe that the presence of an absorbing state forces us to perform ensemble averages in numerical simulations. Therefore, our simulations consist of a large number, n_r, of statistically independent realizations. As for initial conditions, each realization starts with $N/2$ particles of each type uniformly distributed within the patch. Each realization is then followed until the absorbing state ($N_B = 0$) is reached. The interaction distance, R, is chosen to be small compared to the size of the favorable patch but large enough to contain some particles on average ($R\rho > 1$), which provides a lower bound on the minimum number of particles that one can consider, typically $N \gtrsim 20$. In all simulations we set $R = 0.1$, $D = 1$, and $r = 1$ so we have as reference in the continuum limit the nondimensional Eq. (5). Finally, the time step, Δt, is chosen small enough such that the diffusive step is much smaller than the interaction distance (i.e., $\sqrt{2D\,\Delta t} \ll R$). Here we have chosen $\Delta t = 10^{-4}$.

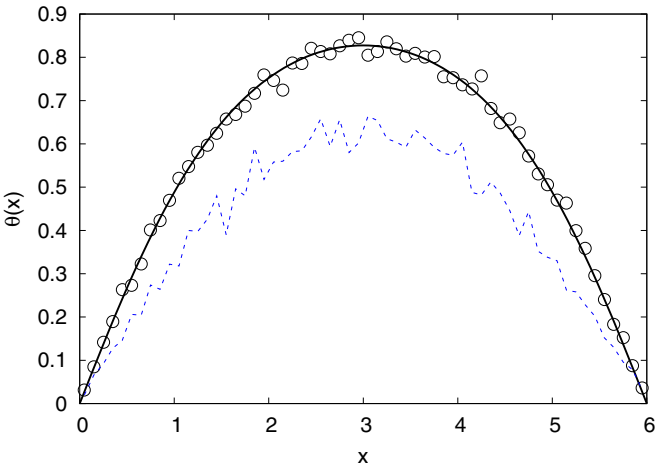

FIG. 1. (Color online) Density field $\theta(x)$ at stationarity for the continuous KiSS model (black solid curve) compared with the local density of B particles, averaged over $n_r = 10$ realizations, in the discrete model (empty circles). The main parameters are as follows: $N = 10^3$, $R = 0.1$, $L = 6$. The (blue) dashed curve represents the local density of B particles obtained with a different model with fixed A particles (see the Appendix for details).

We notice that the model is robust with respect to small changes of R, while if R becomes comparable with the patch size relevant differences arise, as discussed in the Appendix. There, we also briefly consider the subtle effects caused by modifications to the rules specifying the dynamics of the individual-based model.

As an example, we show in Fig. 1 the good agreement, at least for large L, between the stationary population density, $\theta(x,t\to\infty)$, of the continuous KiSS model and the long time (but finite, see Sec. III) particle density, obtained by ensemble averaging the spatial distribution of B particles in the discrete model.

III. THE QUASISTATIONARY STATE

In the discrete model, the presence of an absorbing state ($N_B = 0$) makes population extinction possible for any finite

N, even when $L > L_c$. Nevertheless, the time taken by the system to be absorbed can be very long (for N and L large enough) and, in that case, the system reaches a quasistationary state. The quasistationary distribution is defined as the probability distribution conditioned on nonextinction [25,26,35,36,38,39]. In general, it provides interesting information about the properties of systems with an absorbing state [25,26] but, except in some rare cases, it cannot be evaluated explicitly.

As shown in Fig. 1, the quasistationary distribution, apart from fluctuations, essentially reproduces the results obtained with the continuous model, at least when L and N are sufficiently large. It is then natural to study under which conditions this correspondence holds. In particular, in this section, we focus on the behavior of the biomass per unit length defined as (see Refs. [40,41])

$$\mathcal{B}_C(t) = \frac{1}{L}\int_0^L \theta(x,t)dx. \tag{8}$$

The label C simply recalls that this quantity is defined in the continuum limit and allows to distinguish it from the analogous quantity in the discrete case, for which no labels will be used. We observe that $\mathcal{B}_C(t)$ asymptotically vanishes when $L < L_c$, due to population extinction, and approaches a positive steady value, indicating survival, when $L > L_c$. The asymptotic value $\mathcal{B}_C^\infty = \lim_{t\to\infty} \mathcal{B}_C(t)$ can be used as an order parameter to define the extinction-survival transition.

In the discrete model, the biomass per unit length (8) is nothing but the ratio between the total number of B particles and the total number of particles, $N_B(t)/N$. Since N_B is a time-fluctuating quantity, we consider its ensemble average,

$$\mathcal{B}(t) = \left\langle \frac{N_B(t)}{N} \right\rangle, \tag{9}$$

where the brackets $\langle \cdots \rangle$ denote averaging over different realizations with the same initial conditions and conditioning on survival (i.e., at each time t only the realizations with $N_B(t) \geqslant 1$ are considered). When conditioning on nonextinction, at long times, $\mathcal{B}(t)$ approaches a definite value (Fig. 2) which is the average over the quasistationary distribution.

In the bottom panels of Figs. 2(a) and 2(b) we compare the time evolution of $\mathcal{B}_C(t)$ and $\mathcal{B}(t)$ for two different values of $L > L_c$. For the discrete case we also show, as error bars, the standard deviation of the ratio $N_B(t)/N$,

$$\sigma_{\mathcal{B}}(t) = \langle (N_B(t)/N - \mathcal{B}(t))^2 \rangle^{1/2}. \tag{10}$$

In the top panels, we show the probability, $P_s(t)$ (measured as the fraction of realizations such that $N_B(t) \geqslant 1$ at time t), that the population survived up to time t.

For any given N, when L is large enough [Fig. 2(a)], $\mathcal{B}(t)$ essentially coincides with the continuum limit and all realizations survive [$P_s(t) = 1$ in the observation window] for long times. In these circumstances, the minimal values of $\mathcal{B}(t)$ [lower blue dotted curve in Fig. 2(a)] are well above zero, implying that very unlikely fluctuations are needed to reach the absorbing state. Conversely, as L approaches the critical value L_c [Fig. 2(b)] this is no longer true. As shown in the top panel of Fig. 2(b), $P_s(t)$ exponentially decays to zero at a relatively short time. More importantly, the agreement between $\mathcal{B}(t)$ and the continuum limiting value gets poorer. In particular, at long

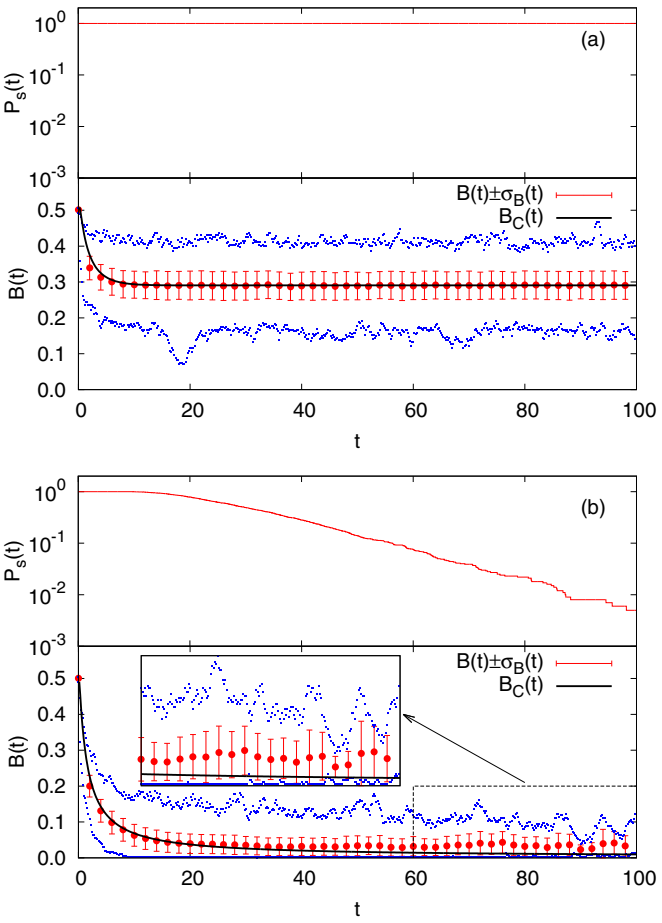

FIG. 2. (Color online) Survival probability and biomass as a function of time for two values of the patch size above the critical value $L_c = \pi$: $L = 4$ (a) and $L = 3.15$ (b), with $N = 400$ particles. Top panels show the survival probability $P_s(t)$, see text. Bottom panels show the time evolution of the continuous [$\mathcal{B}_C(t)$] and discrete [$\mathcal{B}(t)$] biomasses, the error bars on the latter display the standard deviation, $\sigma_{\mathcal{B}}(t)$. The (blue) dotted curves denote the minimum and maximum values of $N_B(t)/N$ observed in all $n_r = 1000$ realizations. The inset in (b) zooms the framed area in the main figure to better show that $\mathcal{B}(t) > \mathcal{B}_C^\infty$ at long times.

times, $\mathcal{B}(t)$ approaches a quasistationary value which is larger than the corresponding continuum one [Fig. 2(b), inset]. This is clearly a consequence of conditioning on nonextinction which leads to an overestimation of the biomass, for these values of the patch size.

The latter observation becomes more quantitative when looking at Fig. 3 where we compare, as a function of $L - L_c$, the limiting value $\mathcal{B}_C^\infty$ with the quasistationary mean value $\mathcal{B}_{\rm QS}$, estimated by averaging $\mathcal{B}(t)$ over the time interval in which it fluctuates around a constant value (see Fig. 2). We have also computed $\mathcal{B}_{\rm QS}$ using the algorithm proposed in Ref. [42], which directly probes the quasistationary distribution, obtaining (not shown) indistinguishable results. The plateau $\mathcal{B}_{\rm QS} \approx \text{const} > \mathcal{B}_C^\infty$, observed when $L \to L_c$, is essentially due to conditioning on nonextinction. The effect is stronger the smaller the number of particles. The dependence of $\mathcal{B}_{\rm QS}$ on the number of particles N clearly demonstrates the departure from the continuum limit when L approaches the critical value.

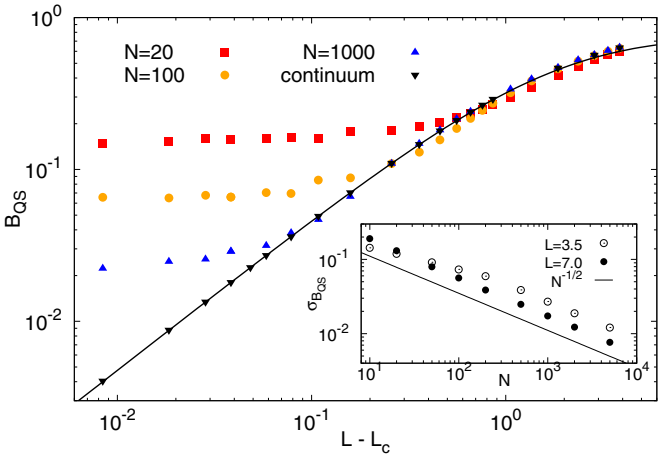

FIG. 3. (Color online) Limiting biomass B_C^∞ and average biomass in the quasistationary state, $\mathcal{B}_{\rm QS}$, as a function of $L - L_c$ for different values of N as in the legend. The solid curve displays $0.75\,\lambda_1$ that corresponds to the behavior in Eq. (11). The factor 0.75 cannot be caught by the argument exposed in the main text. Inset: Standard deviation of the biomass (10) in the quasistationary regime, $\sigma_{\mathcal{B}_{\rm QS}}$, as a function of N for two values ($L = 3.5$ and $L = 7$) of the patch size. The number of realizations used for the averages ranges from 500 to 10 000 depending on the value of N.

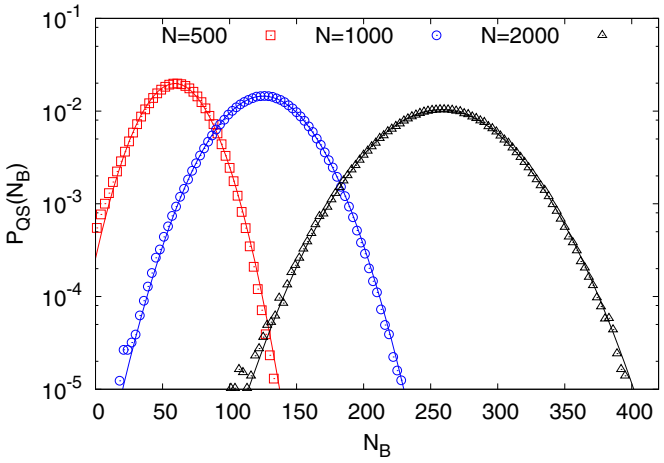

FIG. 4. (Color online) Quasistationary distribution for $L - L_C = 0.3$ and three values of N as in legend. The solid curves display the Gaussian distribution obtained using the mean and standard deviation values measured from data. We observe a fairly good agreement at least for N large enough. When $L \to L_C$ and/or N is not large enough the agreement ceases to be so good, as one can observe from the left tail at $N = 500$.

However, for any $L > L_c$ there exists a value of N (which diverges as $L \to L_c$) above which $\mathcal{B}_{\rm QS}$ tends to the continuous value $\mathcal{B}_C^\infty$.

When the population survives, it is possible to show, using a mean-field-like argument, that the continuous biomass can be approximated by

$$\mathcal{B}_C^\infty(L) \approx \lambda_1, \tag{11}$$

as confirmed in Fig. 3. The idea is to approximate the right-hand side of Eq. (5) as $\partial_x^2\theta + \theta(1 - \overline{\theta})$, where $\overline{\theta}$ denotes the steady-state spatially averaged value. The first eigenvalue of this problem, λ_1^*, is linked to the eigenvalue of the linear KiSS model (4) via $\lambda_1^* = \lambda_1 - \overline{\theta}$. To have a stationary solution one has to impose $\lambda_1^* = 0$, so $\overline{\theta} = \lambda_1$. But at stationarity $\overline{\theta} = \mathcal{B}_C^\infty$, which implies (11). Of course this kind of argument cannot be expected to work when θ is close to 1. It is worth observing that, for $L - L_c \ll 1$, Eq. (11) implies that the continuous biomass is linear in $L - L_c$.

The inset of Fig. 3 shows the standard deviation of the biomass in the quasistationary state, $\sigma_{\mathcal{B}_{\rm QS}}$, at varying N, for two values of L. At least for L and N large enough, the numerical results indicate that $\sigma_{\mathcal{B}_{\rm QS}} \sim N^{-1/2}$. We notice that the inverse square-root dependence of $\sigma_{\mathcal{B}_{\rm QS}}$ on N implies for the standard deviation of the number of B particles $\sigma_N = N\sigma_{\mathcal{B}_{\rm QS}} \sim N^{1/2}$, suggesting that the distribution of N_B particles is Gaussian, as confirmed in Fig. 4. This observation will be exploited in the next section.

IV. CRITICAL PATCH SIZE AND EXTINCTION TIMES IN THE DISCRETE MODEL

In the continuous KiSS model, the critical patch size L_c discriminates between populations able to persist ($L > L_c$) and those doomed to extinction ($L < L_c$). For its ecological importance, many efforts have been devoted to understanding how this critical length is modified in less idealized situations, e.g., taking into account more complex heterogeneous environments [43,44] and/or the presence of external factors like fluid advection [28,41,45,46]. On the other hand, as previously mentioned, in the case of the individual-based model extinction can happen even when $L > L_c$. It is then natural to wonder how the survival-extinction transition of the continuous KiSS model translates in the behavior of the average time to extinction T_e [37], which is linked to the survival probability $P_s(t)$ as $T_e = \int_0^\infty P_s(t)dt$ [47]. Computations of mean extinction times have been mainly carried on in nonspatial models, where the dependence of the extinction time T_e on the number of individuals N at varying the population growth rate has been obtained using diffusive approximations [20]. These results have been influential for their rather simple mathematical formulation and generality. However, it has been recently recognized that the diffusive approximation can give wrong answers [25,35,36].

In what follows we examine the dependence of T_e on the population size N in the extinction ($L < L_c$), critical ($L = L_c$), and persistent ($L > L_c$) regions of the continuous KiSS model. The different regions, indeed, are characterized by unalike functional dependencies of the time to extinction T_e on N as shown in Fig. 5. We observe that, quantitatively, T_e depends on the initial condition; however, the dependence on N and L, which is here explored, is qualitatively independent of the initial condition, provided the initial population is not too small in order to avoid spurious fast extinctions. Therefore, we always considered the initial population $N_B(t = 0) = N/2$. An alternative strategy could be to start from the quasistationary state. However, when N is small and/or $L \leqslant L_c$, as seen in the previous section, the quasistationary state is not so well defined from a physical point of view.

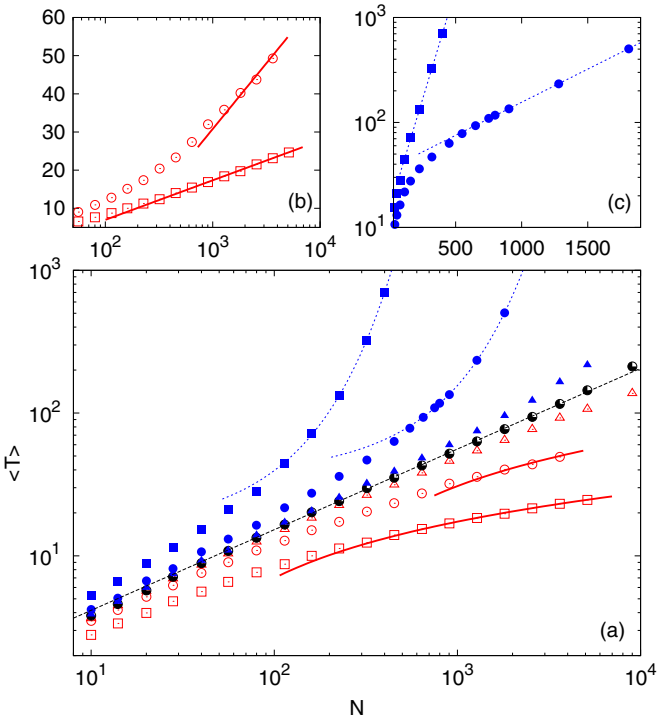

FIG. 5. (Color online) Mean extinction time, T_e, vs population size, N, for different patch sizes $L = L_c + \delta L$. Panel (a) from bottom to top $\delta L = -0.3, -0.1, -0.02, 0, 0.02, 0.1, 0.3$, encompassing the extinction (empty red symbols) and persistence (blue filled symbols) regions, as well as the critical point (black half-filled symbols) of the continuous model. The continuous red lines display the prediction (12) with b' fitted from data; the dashed blue lines correspond to the exponential behavior (14) with a fitted. For $L = L_c$ we found a power-law behavior, $T_e \sim N^{\gamma}$, with best fitting exponent $\gamma = 0.565$ (see text). Panels (b) and (c) display a zoom of the main figure, in appropriate semilog scale, of both the logarithmic (12) and the exponential (14) regime, respectively. We emphasize that the slope in (b) is not fitted but obtained from the first eigenvalue. Depending on the value of N the number of realizations ranges from 500 to 5000.

Let us first consider the extinction region ($L < L_c$). In this case, for the continuous model, extinction is signaled by the density field exponentially going to zero with rate given by the first eigenvalue, $\lambda_1 = 1 - (L_c/L)^2$. In particular, at sufficiently long times we have that the biomass per unit length behaves as $\mathcal{B}_C(t) \sim b\, e^{-|\lambda_1| t}$, with b some constant. In the discrete model, it is natural to assume that extinction will take place at a time T_e such that $\mathcal{B}_C(T_e) \sim 1/N$, implying, apart from a constant b', the logarithmic dependence on N,

$$T_e \sim \frac{1}{|\lambda_1|} \log N + b', \tag{12}$$

which is consistent with the numerics, at least for N large enough (Fig. 5). We observe that the logarithmic behavior (12) is also found in nonspatial models [20].

Conversely, for $L > L_c$, T_e displays an exponential dependence on N (Fig. 5); this is a quite robust feature observed in nonspatial models [20,35,36] where it is derived either with the diffusive approximation or more rigorous large-N approximations (see Ref. [25] for a compact review). Here the spatial extension complicates the use of those well-established techniques. However, we observe that the exponential behavior for the time to extinction is consistent, at least for L and/or N large enough, with the Gaussian behavior of the quasistationary distribution observed in the previous section (see Fig. 4). Indeed, we can assume

$$P_{\rm QS}(N_B) \propto \frac{1}{\sigma_N} \exp\left[- \frac{(N_B - \langle N_B \rangle)^2}{2\sigma_N^2} \right] \tag{13}$$

and it is reasonable to expect that the extinction time will be controlled by the small N_B tail of the quasistationary distribution. Roughly, the idea is that if before the extinction a well-defined quasistationary state sets in, then the extinction will take place when $N_B \approx 1$[1] and the time to reach this state will be proportional to the inverse of its probability so $T_e \sim 1/P_{\rm QS}(N_B \approx 1) \approx 1/P_{\rm QS}(N_B \to 0)$. Hence, using (13) we obtain

$$T_e \sim \sigma_N \exp\left(\frac{\langle N_B \rangle^2}{2\sigma_N^2} \right) \sim \sqrt{N} e^{aN}, \tag{14}$$

where we have used that $\langle N_B \rangle = N \mathcal{B}_{\rm QS}$, with $\mathcal{B}_{QS}$ independent of N (as is true for large N, see Fig. 3), and $\sigma_N = N \sigma_{\mathcal{B}_{\rm QS}} \propto \sqrt{N}$ as from the inset of Fig. 3.

Numerical findings show that the logarithmic and exponential behaviors are separated by the power-law $T_e \sim N^{\gamma}$ at the critical patch size L_c of the continuous model. In particular, our best fit gives $\gamma = 0.565$, which is not far from the analytical estimate $T_e \sim N^{1/2}$ found in nonspatial stochastic logistic models [35,36]. However, while not large, the difference in the value of the exponent is nevertheless clearly measurable and might be due to the spatial structure of the system under study.

We conclude briefly discussing the dependence of T_e on L (Fig. 6). When $L < L_c$, the extinction time T_e is mainly controlled by the eigenvalue λ_1 of the continuous KiSS model. Indeed, from Eq. (12), using the expression of λ_1 we have

$$T_e \sim \frac{L^2}{L_c^2 - L^2} \log N, \tag{15}$$

which is in fairly good agreement with the numerical data when N is large (inset of Fig. 6).

V. CONCLUSIONS

We studied an individual-based reaction-diffusion system of ecological interest. We focused on a model of a discrete population in a favorable patch, surrounded by a deadly environment, which recovers the KiSS model in the continuum limit. The presence of an absorbing state together with demographic stochasticity makes population extinction possible even when the continuous model would allow for population survival. In such a case, however, the system attains a quasistationary state that we have investigated at varying the system and population sizes. We have shown that above the KiSS critical patch size the biomass in the quasistationary

[1] In other terms one assumes that once $N_B = 1$ the extinction takes place with certainty.

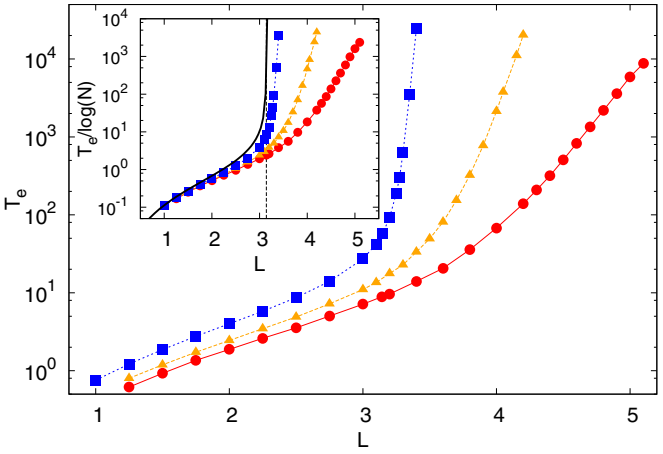

FIG. 6. (Color online) Mean extinction time T_e as a function of the patch size L for $N = 40$ (red circles), $N = 100$ (orange triangles), and $N = 1000$ (blue squares). In the inset $T_e/\log N$ versus L is compared to the asymptotic prediction (15) (solid black curve). The vertical dashed line marks the critical value $L_c = \pi$. The number of realizations used for the averages ranges from 500 to 5000 depending on the value of N.

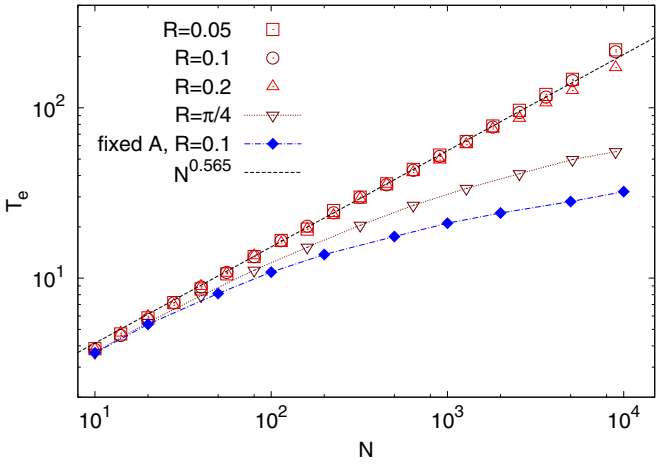

FIG. 7. (Color online) Average extinction time vs N for $L = L_c$ at varying R as from the legend and considering nonmotile A particles. The power-law behavior $T_e \sim N^{0.565}$, identifying the extinction-survival transition, is robust for variations of the interaction distance around the reference value $R = 0.1$; for much larger values ($R = \pi/4$) the critical behavior is considerably altered. The same happens if one considers a model in which particles of type A do not move (filled diamonds).

state recovers the continuum limit value only if the population is large enough. On the other hand, when the population has a small number of individuals, the link between biomasses, defined in the continuous and particle models, ceases to exist. In particular, when the patch size tends to the critical value the number of individuals required to recover the continuum limit diverges.

Moreover, we have shown that the transition from extinction to survival translates, in the discrete model, into the transition from a logarithmic to an exponential dependence of the average time to extinction, T_e, at varying the population size, N. At the transition, these two behaviors are separated by a power-law dependence $T_e \sim N^{\gamma}$ with an exponent definitively different from the analytical prediction obtained in the nonspatial logistic model.

We conclude mentioning that it would be interesting in the future to investigate the effects of population discreteness in more complex heterogeneous environments [43,44] and possibly in the presence of advection [28,41,46]. In such cases, besides the survival-extinction transition, we expect that the discreteness of the population will impact in nontrivial ways on the spatial propagation properties of the population.

APPENDIX: EFFECTS OF CHANGES OF THE MICROSCOPIC RULES OF THE INDIVIDUAL-BASED MODEL

In this Appendix we consider how two different modifications in the individual-based model affect the system dynamics: the first one is concerned with variations of the interaction distance R (in order to check the robustness of the particle model) and the second one is concerned with particles' motility and consists in considering fixed A particles to investigate changes in the continuum limit.

The interaction distance R is a crucial parameter for the individual-based model and it is associated to fluctuations of the number of individuals. A significant variation of R should thus have important consequences, through its impact on the effective growth rate. In Fig. 7 we present a comparison between numerical results obtained in the reference case $R = 0.1$, used in this study, and those obtained with different values of R. For illustrative purposes only, we focus on the average extinction time as a function of N by fixing L at the critical value L_c. As shown in the figure, the power-law scaling $T_e \sim N^{\gamma}$ (with $\gamma \simeq 0.565$), and hence also the value of the critical patch size in the discrete model, is robust if the interaction distance varies within the same order of magnitude ($R = 0.05$ and $R = 0.2$).

The situation differs when R becomes comparable with the patch size: T_e is no longer described by a power law (see the case $R = \pi/4$ in Fig. 7), meaning that the discrete model is no longer at the critical point. Indeed, at large N the curve $T_e = T_e(N)$ bends towards a logarithmic shape as in Fig. 5 when $L < L_c$. Actually, a similar tendency towards smaller values of T_e characterizes the large N behavior for $R = 0.2$, although the effect is so weak that it is difficult to be seen in the figure. The faster extinction is likely due to the fact that increasing R causes the hostile boundary conditions to be felt deeper inside the favorable patch. In other words, while on average the number of particles within R gets larger, the fraction of B particles does not, due to its depletion close to the boundary.

As for the modifications of the motility of particles, we study a case in which A particles are fixed, and the only other change in the particle model is that, in order to preserve the total number of individuals when a B particle is absorbed at the boundary, a new A particle is introduced at a random position (uniformly in the patch). This model has a biological justification in the case in which individuals of type A (the nutrient) are nonmotile (e.g., a plant species) and individuals of type B belong to a motile species feeding on it. The new model

shows a deep alteration in the critical behavior at $L = L_c$ (see the filled diamond symbols in Fig. 7) and the continuum limit of such a model is not given by Eqs. (1) and (2) (see also Fig. 1) because particles of type A and type B do not undergo the same diffusive process. One can expect that in this case the effective growth rate is reduced due to less frequent encounters between individuals of different types—A particles close to the boundaries have fewer chances to turn into B particles, and the extinction times that result are smaller with respect of the original particle model. This highlights once more that the relation between individual-based and continuous reaction-diffusion models is a delicate one, which needs to be carefully taken into account when modeling the evolution of biological populations.

[1] J. D. Murray, *Mathematical Biology* (Springer-Verlag, Berlin, 1993).
[2] G. Flierl, D. Grunbaum, S. Levin, and D. Olson, J. Theor. Biol. **196**, 397 (1999).
[3] A. De Wit, Adv. Chem. Phys. **109**, 435 (1999).
[4] Y. Togashi and K. Kaneko, Phys. Rev. Lett. **86**, 2459 (2001).
[5] T. Tél, A. de Moura, C. Grebogi, and G. Károlyi, Phys. Rep. **413**, 91 (2005).
[6] S. Fedotov, D. Moss, and D. Campos, Phys. Rev. E **78**, 026107 (2008).
[7] Z. Neufeld and E. Hernández-García, *Chemical and Biological Processes in Fluid Flows* (World Scientific, Singapore, 2009).
[8] R. Durrett and S. Levin, Theor. Pop. Biol. **46**, 363 (1994).
[9] E. Brunet and B. Derrida, Phys. Rev. E **56**, 2597 (1997).
[10] D. Panja, Phys. Rep. **393**, 87 (2004).
[11] L. Pechenik and H. Levine, Phys. Rev. E **59**, 3893 (1999).
[12] C. R. Doering, C. Mueller, and P. Smereka, Physica A **325**, 243 (2003).
[13] O. Hallatschek and K. S. Korolev, Phys. Rev. Lett. **103**, 108103 (2009).
[14] L. Geyrhofer and O. Hallatschek, J. Stat. Mech. (2013) P01007.
[15] P. Grassberger, Europhys. Lett. **103**, 50009 (2013).
[16] R. Durrett and S. A. Levin, Phil. Trans. R. Soc. B **343**, 329 (1994).
[17] J. Joo and J. L. Lebowitz, Phys. Rev. E **72**, 036112 (2005).
[18] J. G. Skellam, Biometrika **38**, 196 (1951).
[19] H. Kierstead and L. B. Slobodkin, J. Mar. Res. **12**, 141 (1953).
[20] R. Lande, Am. Nat. **142**, 911 (1993).
[21] V. Méndez, I. Llopis, D. Campos, and W. Horsthemke, Theor. Pop. Biol. **77**, 250 (2010).
[22] V. Méndez, W. Horsthemke, J. Casas-Vázquez, and E. Zemskov, Eur. Phys. J. (Special Topics) **146**, 189 (2007).
[23] C. Escudero, J. Buceta, F. J. de la Rubia, and K. Lindenberg, Phys. Rev. E **69**, 021908 (2004).
[24] S. Berti, C. López, D. Vergni, and A. Vulpiani, Phys. Rev. E **76**, 031139 (2007).
[25] O. Ovaskainen, J. Appl. Prob. **38**, 898 (2001).
[26] R. Dickman and R. Vidigal, J. Phys. A: Math. Gen. **35**, 1147 (2002).
[27] A. Okubo and S. Levin, *Diffusion and Ecological Problems* (Springer, Berlin, 2001).
[28] A. B. Ryabov and B. Blasius, Math. Model. Nat. Phenom. **3**, 42 (2008).
[29] V. Mendez, S. Fedotov, and W. Horsthemke, *Reaction Transport Systems: Mesoscopic Foundations, Fronts, and Spatial Instabilities* (Springer Verlag, Berlin, 2010), Chap. 9.
[30] V. Méndez, C. Sans, I. Llopis, and D. Campos, Math. Biosci. **232**, 78 (2011).
[31] V. Méndez and D. Campos, Phys. Rev. E **77**, 022901 (2008).
[32] J. M. Diamond and R. M. May, in *Theoretical Ecology: Principles and Applications*, edited by R. M. May (Saunders, Philadelphia, PA, 1976), pp. 163–186.
[33] R. S. Cantrell and C. Cosner, J. Math. Biol. **37**, 103 (1998).
[34] R. Cantrell and C. Cosner, Theor. Pop. Biol. **55**, 189 (1999).
[35] I. Nåsell, J. Theor. Biol. **211**, 11 (2001).
[36] C. R. Doering, V. S. Khachik, and L. M. Sander, Multiscale Model. Simul. **3**, 283 (2005).
[37] O. Ovaskainen and B. Meerson, Trends Ecol. Evol. **25**, 643 (2010).
[38] I. Nåsell, Math. Biosci. **156**, 21 (1999).
[39] V. Grimm and C. Wissel, Oikos **105**, 501 (2004).
[40] D. A. Birch, Y.-K. Tsang, and W. R. Young, Phys. Rev. E **75**, 066304 (2007).
[41] D. Vergni, S. Iannaccone, S. Berti, and M. Cencini, J. Theor. Biol. **301**, 141 (2012).
[42] M. M. de Oliveira and R. Dickman, Phys. Rev. E **71**, 016129 (2005).
[43] N. Shigesada, K. Kawasaki, and K. Teramoto, Theor. Pop. Biol. **30**, 143 (1986).
[44] N. Kinezaki, K. Kawasaki, F. Takasu, and N. Shigesada, Theor. Pop. Biol. **64**, 291 (2003).
[45] E. R. Abraham, Nature **391**, 577 (1998).
[46] K. A. Dahmen, D. R. Nelson, and N. M. Shnerb, J. Math. Biol. **41**, 1 (2000).
[47] S. Redner, *A Guide to First-Passage Processes* (Cambridge University Press, New York, 2001).